ORIGINAL ARTICLE

Thermal conversion behavior of cellulose and hemicellulose fractions isolated from tea leaf brewing waste: kinetic and thermodynamic evaluation

Şeyda Taşar[1] (ID)

Abstract

This study aims at investigating the thermal decomposition process (pyrolysis) of tea leaf brewing waste (TLBW) and its main component (hemicellulose, cellulose) under non-isothermal conditions and these pyrolysis process kinetic/thermodynamic parameters. Hemicellulose (TLBW-H) and cellulose (TLBW-C) were isolated from the TLBW with delignification process. The isolation effectiveness was discussed and interpreted according to structural analysis (FTIR) results. The fuel analysis (proximate and ultimate), chemical analysis, and structural analysis (FTIR) of the tea leaf brewing waste and its main component were carried out. The thermal analysis (TGA and DTG) of TLBW, TLBW-H, and TLBW-C was investigated under a nitrogen gas atmosphere of 10 ml/min in the temperature range of 25–900 °C. Kinetic and thermodynamic parameters were calculated using Coast–Redfern (CR) model and main thermodynamic equations. A fourteen solid-phase theoretical degradation reaction model was then applied to evaluate the TGA results of the samples. Active pyrolysis started after 210 °C and ended at 527 °C for TLBW-H, 538 °C for TLBW-C, and 602 °C for the TLBW. For the total decomposition steps, the best model equation representing the degradation was found to be the chemical kinetic equation F(3) for all of the samples. Using the model equation that best represents the degradation, the activation energies and ln (A min-1) calculated from the thermal decomposition kinetics of raw tea brewing waste, hemicellulose and cellulose were determined as 46.71-14.42-23.84 kJ/mol and 7.67-13.41-11.92, respectively. As a result, it is predicted that the kinetic and thermodynamic parameters calculated in this study will be useful in terms of the pyrolysis process of TLBW and its main component and the design of pyrolysis reactors.

Statement of novelty

- This is a research on the thermal decomposition behavior and kinetic analysis of tea leaf brewing waste and its main components (cellulose and hemicellulose).
- Activation energy was estimated for 14 different theoretical solid-phase decomposition model equations using the Coast–Redfern method.
- Important thermodynamic parameters for the pyrolysis process were calculated and compared.
- The findings will be useful for the thermal degradation process design of TLBW and its main components.

1 Introduction

The limited reserves of fossil energy resources and the fact that they cause environmental pollution (global warming) have required the programmatic limitation of their use. Therefore, in recent years, the process and reactor design for clean energy generation from waste lignocellulosic biomass resources came to the fore. Biomass wastes can be used directly as an alternative energy source. However, their energy content is low due to their high moisture and oxygen content. Conversion processes are used to improve the fuel quality of biomass resources. One of these processes is the pyrolysis process. Pyrolysis, one of the thermochemical conversion methods, is more

✉ Şeyda Taşar
  sydtasar@hotmail.com; sydtasar@firat.edu.tr

[1] Department of Chemical Engineering, Firat University, 23279 Elazig, Turkey

effective and eco-friendly than other thermochemical conversion methods [1, 2].

The chemical structure and composition of lignocellulosic biomass resources are different from each other. The basic components of lignocellulosic biomass sources are cellulose, lignin, and hemicellulose. Cellulose and hemicellulose formed the cell wall. They are polysaccharides with high hydrogen and oxygen content. Lignin is the key component that tightly binds these cell walls together. It is a high carbon-containing phenolic polymer. Apart from these, components that can be dissolved in suitable solvents in the biomass are termed extractive matters [3]. Cellulose is insoluble, linear, and unbranched homopolysaccharides composed of 1,4-β-glycosidic bonds. It is the most common glucose biopolymer in the structure of biomass [4]. In the structure of hemicellulose, there are five-carbon sugars (D-xylose and L-arabinose) and six-carbon sugars (D-galactose, D-glucose, and D-mannose), as well as uronic acid, 4-O methyl glucuronic acid, and galacturonic acid residues [5]. Lignin is a polyphenolic macromolecule. Contrary to other polysaccharides, it is a three-dimensional polymer, and, as a result, it acts as a binder [6]. Lignin macromolecule contains coniferyl alcohol, sinapyl alcohol, and a minor quantity of p-coumaryl alcohol [7].

Thermal degradation of biomass works by a complex reaction mechanism involving parallel and sequential reactions known to occur at different speeds. The kinetic parameters of these complex reactions change with pyrolysis conditions and the chemical composition of biomass resources [8, 9]. The pyrolysis activity of a biomass's main constituents is very different from each other [10]. Hemicellulose, cellulose, and lignin show active degradation in different temperature ranges. The active decomposition temperature of hemicellulose which is the most heat-sensitive component of the plant structure is specified as 200–260 °C. Lignin degrades at a higher temperature (between 280 and 500 °C) than cellulose and hemicellulose [11].

The pyrolysis process is a solid-state degradation, and its kinetic parameters are determined by thermoanalytical methods. To expose the pyrolysis behavior and the kinetic and thermodynamic parameters, the thermogravimetric analysis (TGA) approach can be used [12, 13]. TGA analysis is significant for the pyrolysis process design, optimization of thermochemical conversion processes, feasibility of operation and processes, and scaling for industrial manufacturing [14].

In the TGA method, the total reaction kinetics or degradation kinetics and kinetic parameters for the degradation steps representing the degradation of the main components can be determined separately by using the weight loss data during the decomposition of solids because the shape of the curve obtained due to the weight reduction as a result of the thermogravimetric analysis is a function of the reaction kinetics. Different methods are used to determine the kinetic variables using this curve. These methods are grouped as integral methods that use weight change with temperature directly, differential methods using weight change rate, difference differential methods where second differences in weight change rate are taken into account, and special methods that can be applied to the first velocities.

Tea *Camellia sinensis*, a plant species that is a member of the tea family Theaceae, can grow in humid climates, and its leaves and buds are used for beverage production. Tea production is carried out only in the Eastern Black Sea Region in Turkey including Rize, Trabzon, Artvin, Giresun, and Ordu on a rugged land of 785 thousand decares according to 2019 data. According to a statistical report published by tea manufacturers (Çaykur enterprises report 2019 [15]), 270 thousand tons of dry tea are produced each year in Turkey. According to the global tea statistics report (2019) [16], Turkey ranks sixth in production among tea-producing countries, including China, Sri Lanka, Georgia, Kenya, Indonesia, and Iran, and first in annual consumption per person. Accordingly, the consumption of tea is approximately 3.5 kg per person per year in Turkey.

Tea leaf brewing waste is a lignocellulosic biomass waste that is produced as a result of the tea brewing process that can be grouped as both domestic and industrial waste. The conclusion reached in the light of statistics reports is that the reserve of tea brewing waste is high and it is a waste that should be evaluated. Nevertheless, the waste (tea leaf brewing waste (TLBW)) does not yet have an economic value and has an acceptable area of application/use. In recent years, a new field to use tea leaf brewing waste with economic added value has been opened: the production of worm compost. However, this is also a very limited sectoral usage area. Although there were considerable investigations on the thermal kinetics of biomass wastes [17–20], there is no detailed data on the pyrolysis reaction kinetics of tea leaf brewing waste and its main component.

In the present study, the pyrolysis behavior of TLBW and its main component was investigated using TGA analysis. The analysis was performed at short interval heating rates (10 °C.min⁻¹) to clearly explain the thermal degradation phenomenon. The kinetic and thermodynamic parameters were calculated for fourteen solid-phase decomposition theoretical reaction models. The physicochemical characteristics of the tea leaves' brewing waste and its main components were determined by FTIR, ultimate and proximate analysis.

2 Material and methods

TLBW used in this study was obtained from local tea houses in Elazig, Turkey. The obtained TLBW was dried firstly under

ambient conditions in the laboratory and then 48 h in an oven at 80 °C. Further, TLBW was ground using a food mill (brand of Renas) and blended to form a homogeneous mixture. The homogeneous mixture was separated into different particle sizes using a lab-scale vibrating screen series. These fractions of various particle sizes were kept in polyethylene lidded containers for use during the experiments. All of the chemicals used for this experimental research (isolation of hemicellulose and cellulose) are of analytical purity.

2.1 Isolation of cellulose and hemicellulose

The sodium chlorite delignification process was used commonly to recover of hemicellulose and cellulose fractions from wheat straw [21], air-dried sugarcane bagasse [22], and silvergrass [23] in the previous studies. Isolation stages of hemicellulose and cellulose from the tea leaf brewing waste were schematized in Fig. 1.

Dewaxed step The tea leaf brewing waste (20 g) fraction of −30 +50 mesh particle size was treated with distilled water. This process was carried out in a water bath at 60 ° C and 120 rpm agitation speed for 6 h, with a solid-to-liquid ratio (w/v:g/ml) of 1:10. After washing with water, the solid residue was filtered and dried in the oven at 60 °C for 12 h.

Then the dried solid residue sample was extracted with a mixture of toluene/ethanol (v/v: 2/1) for 6 h using a Soxhlet extractor to remove the oil, wax, and resins contained in the dried solid residue. The solid residue remaining in the cartridge after extraction was dried in an oven at 60 °C for 12 h. As a result of this process, a sample free of extractives was obtained.

Delignification step To isolate the lignin contained in the waste that was free of extractives, the sample was treated with 6 % $NaClO_2$ for 2 h at 75 °C. During the treatment process, the pH of the medium was tried to be kept constant at 3.5–3.8 using 6 M acetic acid. The solid residue (i.e., insoluble part) obtained as a result of the delignification process was holocellulose (cellulose + hemicellulose). The soluble fraction was the filtrate containing lignin. The pH of the filtrate was adjusted to about 1.5–1.8 with a 4 M HCl solution; lignin was

precipitated by adding 3 times the volume of ethanol. Lignin was separated from the liquid by centrifugation. The resulting lignin was washed at least three times with ethanol and dried in an oven at 80 °C.

Alkaline pretreatment step The holocellulosic fraction was treated with 10 % NaOH solution for 10 h at 20 °C. The experiment was used at solid-to-liquid ratio (w/v:g/ml) 1:10 and process temperature 25 °C. Afterward, the filtrate including hemicelluloses (alkali-soluble fraction) and cellulose (alkaline-insoluble fraction) was separated from each other. The cellulosic fraction was washed with distilled water and dried in an oven at 80 °C. The pH value of the filtrate (contained hemicellulose) was brought to about 5.0–5.5 with a 4 M HCl solution. Then to the precipitation of hemicellulose, ethanol (3 times the amount of filtrate) was added to the filtrate. The hemicellulosic precipitate occurred and separated. The centrifuge was used for these separation processes. The isolated hemicellulose was washed with ethanol at least five times and dried in an oven at 80 °C.

2.2 Psychochemical characterization of the tea leaf brewing waste and its main component

Ultimate analysis The amounts of carbon, hydrogen, nitrogen contained in the TLBW, and its main component were measured using an elemental analyzer (a Leco CHNS-932). Only oxygen content was calculated from the difference.

Proximate analysis The ash and volatile matter amounts of the tea waste were determined according to ASTM-D1102 [24] and ASTM-E872 [25] standards, respectively. The moisture determination of the TLBW and its main components were determined at 80 °C in the Mettler LJ16 moisture analyzer. Proximate analysis experiments were performed using samples with a particle size of 154 μm (less than 100 mesh). All of the analysis was repeated at least three times, and the calculation results were presented by taking the average of the experiments.

Chemical analysis The chemical composition (extractive substance. hemicellulose, lignin, and cellulose) of TLBW was determined by using analytical methods [26]. All of the
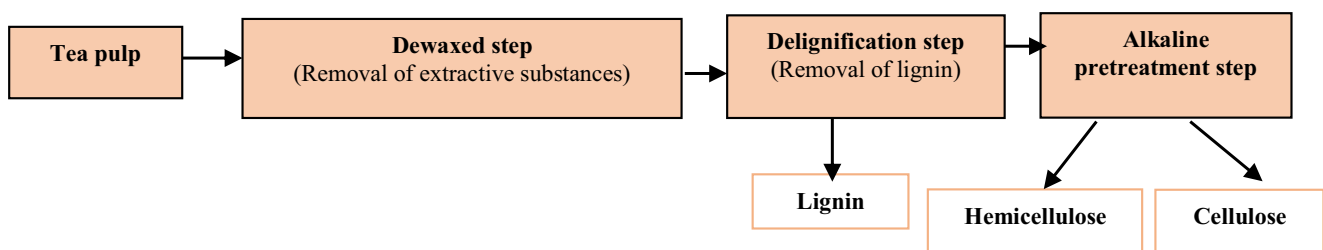

Fig. 1 Isolation stages of hemicellulose and cellulose from the tea leaf brewing waste

analysis was repeated at least five times (only cellulose content was calculated from the difference), and the calculation results were presented by taking the average of the experiments.

Fourier transform infrared resonance (FTIR) spectrum FTIR analysis was carried out to determine the functional groups in the structure of hemicellulose and cellulose obtained by isolation from TLBW and raw material and to discuss the efficiency of the isolation process. For this purpose, Shimadzu IR Spirit spectrophotometer was used, and measurements were carried out using 45 scans in the range of 400 to 4000 cm^{-1}. A background scan was performed to prevent interference from airborne components, and samples were scanned under the same conditions.

Thermogravimetric sanalysis The thermal decomposition behavior of tea leaf brewing waste, isolated hemicellulose, and cellulose was investigated under a nitrogen gas atmosphere of 10 ml/min in the temperature range of 25–900 °C. Experiments using 10 mg of sample were carried out with a Shimadzu TA 60-WS brand thermal analyzer. Using the thermograms obtained, both the thermal degradation behavior of the samples was revealed, and the kinetic and thermodynamic parameters of the thermal degradation processes of the samples were calculated and interpreted.

2.3 Kinetic studies

Although the thermal decomposition process of biomass involves a very complex series of reaction steps, many researchers have done kinetic analysis by considering the following basic reaction. The kinetic modeling was made by taking this basic equation into account; reaction parameters (activation energy and exponential constant) were calculated and interpreted. In this study, the following general equation was used [27]:

$$aA(solid) \rightarrow bB(solid) + cC(volatile) \tag{1}$$

If it is accepted that the conversion of biomass resources to product is a one-step reaction [28], the rate of decomposition of solid matter is expressed as in Eq. 2:

$$\frac{dx}{dt} = k(T) f(x) \tag{2}$$

Here; x transform fraction ($x = \frac{mi-mt}{mi-ms}$), t time, k speed constant, and f(x) are the solid-phase decomposition theoretical model equation. If the heating rate ($Q = \frac{dT}{dt}$) and the rate constant $k = A\exp\left(\frac{-E}{RT}\right)$ are replaced in the general Eqs. 3 and 4, then the equations are obtained:

$$\frac{dx}{dT} = \frac{A}{Q} f(x)\exp\left(\frac{-E}{RT}\right) \tag{3}$$

Coats–Redfern methods Different methods are used to calculate the results of this problematic equation because its methodical solution is impossible. Among the methods developed by various researchers to determine kinetic variables from the data obtained as a result of the thermogravimetric analysis, the Coast–Redfern method (C-R) [29], which takes into account integral analysis and is widely used to find kinetic parameters, was used in the present study [3; 28]. The Coats–Redfern method required an assumption to be made regarding the value of the reaction order for g(x).

If the integral of Eq. 3 is taken, Eq. 4 is obtained:

$$g(x) = \int \frac{dx}{f(x)} == \frac{A}{Q} \exp\!\int \left(\frac{-E}{RT}\right) dT \tag{4}$$

where A, E, R, and T are the frequency factor, the activation energy, the ideal gas constant, and the absolute temperature (K), respectively.

The frequency factor A and the heating rate are taken out of the integral since they are not a function of temperature:

$$g(x) = \int \frac{dx}{f(x)} \frac{A}{Q} = \exp\!\int \left(\frac{-E}{RT}\right) dT \tag{5}$$

Equation 5 is obtained that the expression ($\int\exp\left(\frac{-E}{RT}\right)$ does not specify the integral, so if the right side of the equation opens to an asymptotic series and the higher terms are neglected,

$$\frac{g(x)}{T^2} = \frac{AR}{QE} \left(1 - \frac{2RT}{E}\right) \exp\left(\frac{-E}{RT}\right) \tag{6}$$

equality is obtained. If $\frac{2RT}{E} << 1$ is accepted and the natural logarithm of both sides of the equation is taken the final equation (general equation), we used to calculate the kinetic parameter for different solid-state kinetic models:

$$\ln\left(\frac{g(x)}{T^2}\right) = \ln\left(\frac{AR}{QE}\right) - \left(\frac{E}{RT}\right) \tag{7}$$

The $\ln\left(\frac{g(x)}{T^2}\right)$ values are plotted against -1/T, and the line equation is determined. The activation energy was calculated from the slope of the line equation obtained, and the frequency factor was calculated from the shift value.

Different solid-phase decomposition theoretical models have been developed to express the degradation reactions of solids [30, 31]. Considering fourteen different theoretical solid-phase decomposition kinetics model equations, the theoretical model equation that best represents the thermal decomposition kinetics was tried to be determined. The solid-

phase decomposition theoretical models used in the study are given in Table 1.

2.4 Thermodynamic analysis

To determine the realization potential of the thermal degradation process, some thermodynamic parameters (ΔH, ΔG, and ΔS) need to be calculated [32]. The equations used in the calculation of these parameters were presented [28, 33–35]:

$$A^* = \frac{x.E.\exp\left(\dfrac{E}{R.T_p}\right)}{R.T_p^2} \tag{8}$$

$$\Delta H = E - RT \tag{9}$$

$$\Delta G = E + R.T_p.\ln\left(\frac{K_B T_P}{h.A}\right) \tag{10}$$

$$\Delta S = \frac{\Delta H - \Delta G}{T_P} \tag{11}$$

where T_p, h, and K_B represent peak temperature (K) in the DTG curve, Plank constant (6.626×10^{-34} J s), and Boltzmann constant (1.381×10^{-34} J.K^{-1}), respectively.

3 Results and discussion

3.1 Physicochemical analysis

The physicochemical properties of tea brewing waste and the main components isolated from this waste by the delignification method are summarized in Table 2. The examination of the proximate analysis results determined that TLBW and its main components (hemicellulose and lignin) contained less than 5% moisture. The applicability of thermal conversion processes (especially pyrolysis and combustion processes) depends on the moisture content. As the moisture content increase, heat loss increases. Thus, the moisture content should be below 10%. Therefore, it was concluded that the selected raw material resources were suitable for the thermal transformation process. On the other hand, the samples had a high content of volatile matter (in the range of 73.65–75.43% by weight) and a small amount of ash content (in the range of 0.96–3.83% by weight). The comparison of proximate compositions of biomass samples with other biomass samples known to have the lignocellulosic structure in the literature showed that they had similar characteristics [36, 37].

The fuel value of biomass is largely related to its upper calorific value. The upper calorific values are generally used to compare the biomass resources to be used as fuel. The proximate contents of biomass resources are important parameters that directly affect the combustion process. Biomass sources with high ash content are less desirable than fuels, while biomass sources with high fixed carbon content are more preferred. The ash content increases the operating cost and increases the amount of waste that needs to be disposed of resulting in low-energy conversion because the ash content (inorganic substance contents) of biomass sources reduces oxygen diffusion during the combustion process and reduces the combustion efficiency [38, 39].

It is anticipated that the tea brewing waste and the basic components gained by insulation will cause high ignition performance. It was found that TLBW and its main components had high volatile matter content, high upper heat value

Table 1 The reaction models of the solid-phase decomposition to determine the activation energies [30, 31]

Models	f(x)	g(x)
Chemical kinetics F(0)	1	x
Power law (P1)		
One-dimensional interaction geometry (R1)		
Chemical kinetics (1/2)	$(1-x)^{1/2}$	$\left[1-(1-x)^{1/2}\right]$
Interaction geometry in cylindrical system (R2)		
Chemical kinetics (2/3).	$(1-x)^{2/3}$	$\left[1-(1-x)^{1/3}\right]$
Interaction geometry spherical system (R3)		
Chemical kinetics F (1)	$(1-x)$	$-\ln(1-x)$
Chemical kinetics F (2)	$(1-x)^2$	$(1-x)^{-1}-1$
Chemical kinetics F (3)	$(1-x)^3$	$\left[(1-x)^{-2}-1\right]/2$
Parabolic law (D1)	$1/2x$	x^2
Holt–Cutler–Wadsworth equation (D2)	$1/-\ln(1-x)$	$[(1-x)\ln(1-x)]+x$
Jander equation (D3)	$3 \times (1-x)^{2/3}/2 \times \left[1-(1-x)^{1/3}\right]$	$\left[1-(1-x)^{1/3}\right]^2$
Ginstling–Brounshtein equation (D4)	$3/2 \times \left[(1-x)^{1/3}/1-(1-x)^{1/3}\right]$	$1-\left(\frac{2x}{3}\right)-(1-x)^{2/3}$

Table 2 Physicochemical characteristics properties of TLBW and its main components

Physico-chemical characteristics	TLBW	TLBW-H	TLBW-C
	Value (wt. %)	Value (wt. %)	Value (wt. %)
Ultimate analysis			
C	48.55	45.80	48.18
H	5.824	4.083	4.600
N	3.474	-	<0.25
O*	42.15	50.12	46.97
S	-	-	-
Proximate analysis			
Volatile matter (VM)	73.65	74.61	75.43
Ash (A)	3.420	3.830	0.960
Moisture (M)	3.700	4.240	3.870
Fixed carbon (FC)	19.23	17.32	19.74
Chemical analysis			
Hemicellulose (HC)	37.20		
Cellulose (C)	24.93		
Lignin (L)	24.42		
Extractive matters (EM)	10.03		

$O^*(\%wt) = 100 - (\%C + \%H + \%N + \%S)$

(HHV= −13.173 + 0.416VM kJ/g), and high heat generation during the combustion process.

The chemical compositions and morphological structures of biomass resources are quite different from each other. It is known that biomass resources contain hemicellulose, cellulose, and lignin in different composition ratios depending on their structure, age, and growing conditions (climate and environmental factors) [40]. Table 2 shows that the TLBW contains cellulose (24.93%) and hemicellulose (37.20%) of high amount and a lower percentage of lignin (24.42%). The total cellulose and hemicellulose (holocellulose) content was 62.13% which indicates that the TLBW is suitable for biofuel production. The comparison of the chemical analysis results of tea brewing with the biomass samples known to have a lignocellulosic structure available in the literature shows that it has characteristically similar properties [41–44].

The results of the final analysis summarized in Table 2 show that the elemental carbon contents of TLBW and its

main component were high (in the range of 48.55–45.80%). The oxygen content (O*) of TLBW was calculated from the difference. This result is consistent with the results of proximate analysis and shows that it can be evaluated as a biofuel. The ultimate analysis results of the samples are in agreement with similar biomass sources in the literature.

3.2 FTIR analysis

The FTIR spectrum of the TLBW in Fig. 2a presented very wide-ranging and extensive peaks. It showed the presence of -OH groups of peak phenols and alcohols at 3425 cm^{-1}. This peak was due to the –OH groups in the cellulose and lignin molecules known to be present in the tea leaf brewing waste. The peak aliphatic -CH$_3$, =CH$_2$ groups at 2930–2862 cm^{-1} indicated the asymmetric C-H stretching of the 1731 cm^{-1} hemicellulose C=O stretch vibration. One thousand six hundred twenty-eight cm^{-1} represented the tensile vibration of the

C=O bond of the carbonyl groups of lignin and the stretch vibration of ethylene (-C=C-) in the aromatic ring structure of 1517 cm^{-1} lignin. One thousand four hundred forty-six cm^{-1} aliphatic (-CH$_3$) group denotes C-H deformation vibration, originating from the aliphatic parts of lignin. Other peaks were seen in the structure 1382 cm^{-1}; aliphatic C-H bending vibration of methyl and phenyl alcohols, 1267 cm^{-1}; C-O stretch vibration in the ring structure of lignin and xylene, 1033 cm^{-1}; represents the C-OH stretch vibration of cellulose and hemicellulose. The 875 cm^{-1} peak was due to out-of-plane aromatic C-H stretching vibration. It was concluded that TLBW had peaks that were similar to those of other biomass sources such as moso bamboo [45], bamboo powder [46] and barley straw [47] that have lignocellulosic structures and tea waste [48, 49].

Figure 2b shows the FTIR spectrum of hemicellulosic fractions. It refers to the broadband hydroxyl stretching at 3434 cm^{-1}. Peaks in the 2849–3000 cm^{-1} region of the spectrum show the C-H tension in the methyl and methylene groups. Bands of typical xylan structure were observed between 1175 and 1000 cm^{-1}. The tensile and bending bands of C-O, C-C, and C-O-C bonds were concentrated around 1040 cm^{-1}. Similar peaks were observed for the hemicellulosic fraction in studies conducted by Briennzo et al. (2009) [50] and Buranov and Mazza (2008) [51]. One thousand forty-three cm^{-1} is the typical xylan peak, indicating C-O and C-C stresses and the presence of glycosidic bonds. Corresponding to the ring frequency, the sharp band observed at 801 cm^{-1} is attributed to the (p → glycosidic (1 → 4)) bonds between the xylose units in the hemicellulose structure [52].

Fig. 2 FTIR spectrum of TLBW and its main component **a** TLBW, **b** hemicellulosic fraction, and **c** cellulose fraction
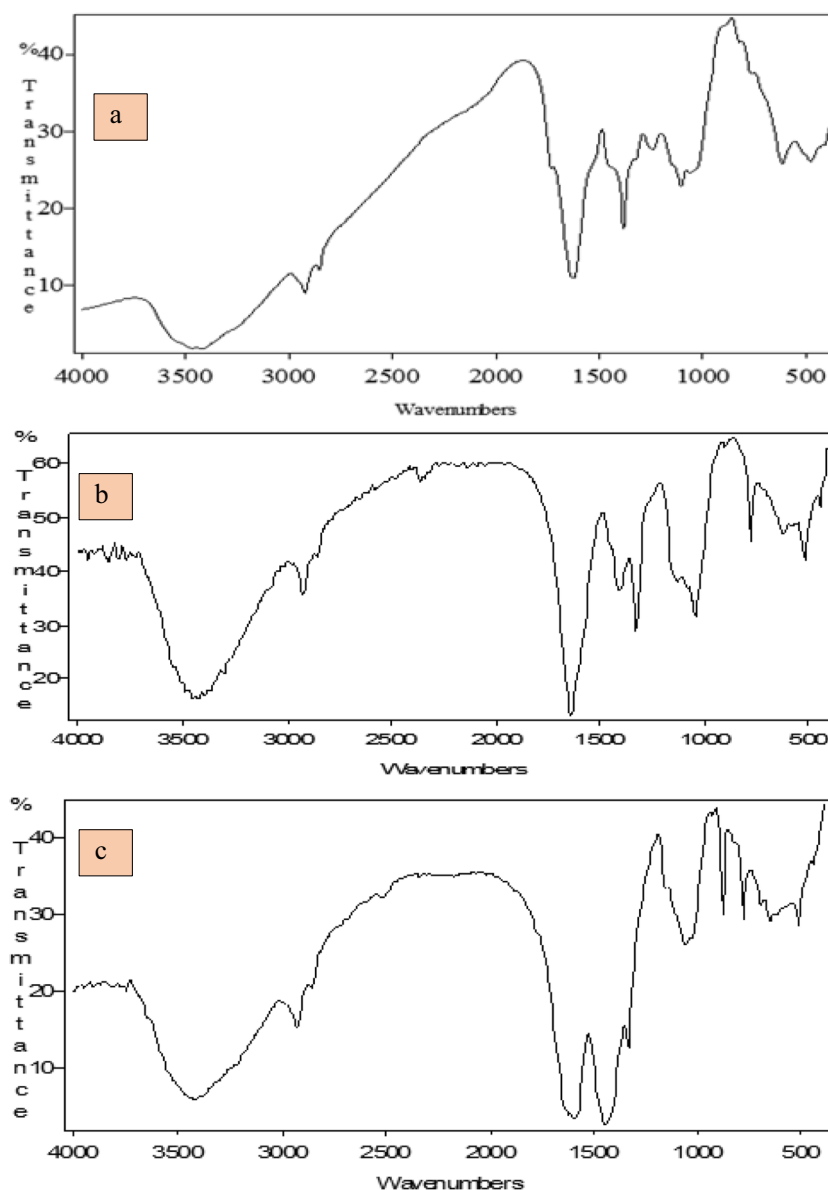
The bands observed at 1648 cm^{-1} belong to the functional group C=O. The fact that this band was located in the region lower than 1700 cm^{-1} was explained with the water absorption of the structure [51]. Peaks between 1473 and 1329 cm^{-1} represent the -CH and -CO twist or stretch frequencies.

The peak at 1246 cm^{-1} was due to carbonyl groups in uronic acid or acetyl groups attached to hemicelluloses. Two small peaks at 910 cm^{-1} indicated the presence of arabinose side chains [52]. The absence of two defining peaks at 1534 and 821 cm^{-1}, indicating the presence of lignin's aromatic skeleton, showed that lignin was aromatic. It demonstrated that the skeleton was absent, that is, the lignin had been completely removed from the hemicellulosic part. These two basic peaks were emphasized in the explanations made by Xiao et al. (2011) [52] and Egüés (2013) [53] regarding the purity of the hemicellulosic structure.

Figure 2c shows the FTIR spectrum of cellulose fractions. The flat band seen around 3334 cm^{-1} expresses the O-H stretching. In the studies conducted by Seki et al. (2013) [54] and Rahman et al. (2015) [55], it was stated that this band belongs to the O-H groups that are found together with hydrogen bonds between the repeating units in the cellulose matrix. The peak seen at 2936 cm^{-1} expresses the characteristic C-H stretching. The presence of =CH$_2$ and -CH$_3$ vibrations was understood from the 2869 cm^{-1} absorption band. This peak was interpreted as the C-H groups' tension of α-cellulose [56]. The sharp band at 1628 cm^{-1} belongs to the C=O functional group. The C-O-C stretch in the pyranose ring at 1067 cm^{-1}, bands between 900 and 1197 cm^{-1} represent various C-O, C-C, C-O-C stretch, and C-O-H bending bands. The band seen around 892 cm^{-1} proves the presence of β-glycosidic bonds in the cellulose molecule. These observed bands seem to be quite compatible with the cellulose bands mentioned in the literature [57]. The absence of a band representing the presence of xylan around 1040 cm^{-1} in the spectrum indicates that the cellulosic structure does not contain xylan, but the presence of the 1446 cm^{-1} band indicates that the isolated α-cellulose had slightly hemicellulosic fractions. Similar comments were made on the existence of these two peaks in the study conducted by Lan et al. (2011) [58].

## 3.3 Thermal degradation of TLBW and its main component

Among the three basic components that make up the structure of biomass, hemicelluloses are the most sensitive to heat. It decomposes in the temperature range of 200–260 °C [59]. Cellulose gives thermal decomposition reactions at temperatures above 300 °C. Lignin thermal stability is higher than other basic components. Lignin undergoes thermal degradation at higher temperatures (between 280 and 500 °C) than cellulose and hemicellulose.

Cellulose initially undergoes gradual degradation, fragmentation, and clarification (solidification) reactions at low temperatures. Then, a rapid gas product formation occurs with the formation of levoglucosan at high temperatures. Degradation reactions that occur first include depolymerization, hydrolysis, oxidation, dehydration, and decarboxylation reactions [60]. Hemicellulose undergoes thermal degradation in two stages. These steps can be expressed as the degradation of the polymeric structure into soluble components and the conversion of monomer units to volatile products by further degradation. Compared to cellulose, hemicelluloses give more gas product, less tar, and char. Unlike cellulose, levoglucosan formation is not observed in these series of reactions. Instead, the tar contains acetic acid, formic acid, and a few furfural derivatives as the main components [61]. Lignin thermal degradation solid (char) product yield is higher than the pyrolysis of cellulose [59]. However, due to the macromolecular structure in which many aromatic units come together with a great variety, no component can dominate the other and become a basic product.

Aqueous distillate recovered after pyrolysis contains methanol, acetic acid, acetone, and water. Tar consists mainly of phenolic components such as phenol guaiacol 2,6-dimethoxyphenol. The gas product contains methane, ethane, and CO$_2$ and accounts for about 10% of lignin. The thermal degradation behaviors of the TLBW and the main components (hemicellulose and cellulose) under an inert atmosphere were investigated by TGA-DTA analysis. The analysis was performed three times, and the average values were compiled. When the thermograms presented in Fig. 3a are examined, the main difference-similarities between the degradation characteristics of isolated main components (hemicellulose, cellulose isolated) by delignification of TLBW and TLBW can be understood.

Figure 3a showed that the raw tea brewing waste passed through three basic separation steps. These were dehydration step (up to 134 °C), evaporation step (248–366 °C), and the coal formation step (> 366 °C), respectively. In the first degradation step which lasted up to a temperature of 134 °C, low molecular weight compounds and water molecules were removed from the structure. The fastest and highest weight reduction occurred in the second zone. This zone is called the active pyrolytic zone. The starting and ending temperatures of the second zone were 248 and 366 °C, respectively. It is stated that the thermal decomposition of hemicellulose and cellulose took place in this temperature range. In parallel with the increase in temperature in this region, lower molecular weight products, i.e., volatile matters, were formed by degradation of hemicellulose and cellulose. The volatile formation was the result of simultaneous exothermic reactions. In this step, hemicellulose, cellulose, and lignin were degraded, respectively. The maximum conversion in the second decomposition zone in the temperature range of 248 °C to 366 °C was

Fig. 3 TGA and DTA curves of TLBW and its main component
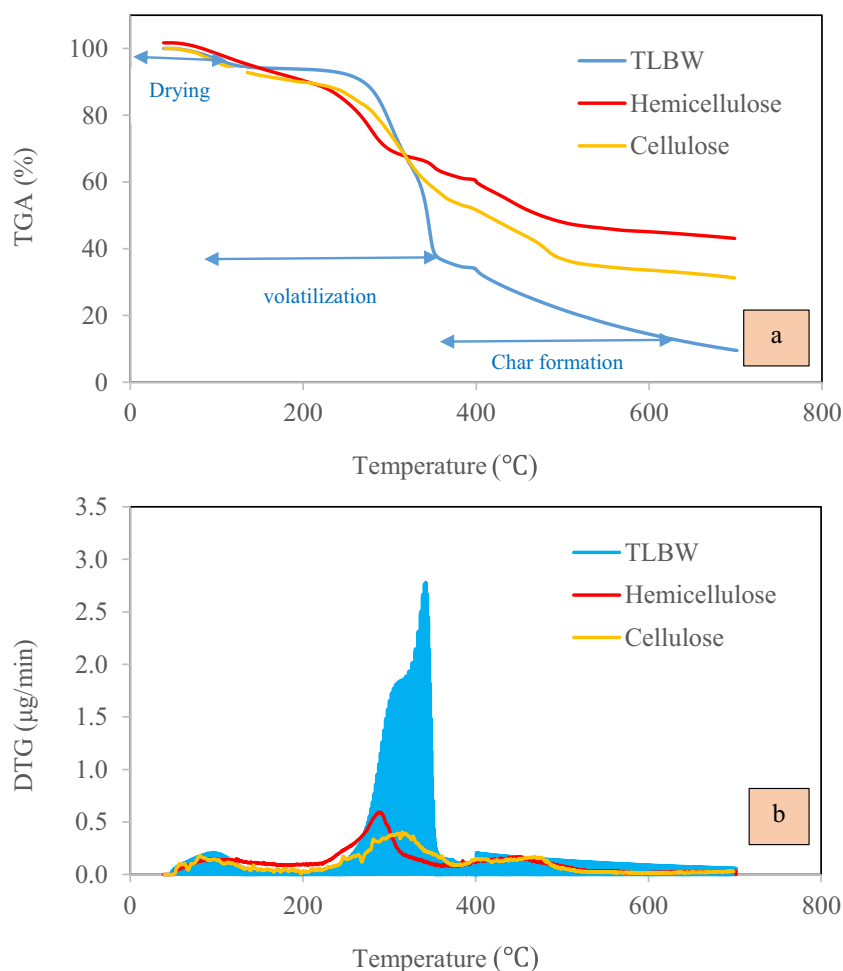
obtained as 40%. The third degradation step observed at a higher temperature (> 366 °C) in the thermogram of TLBW in Fig. 3a represents the degradation of lignin and is an endothermic event.

Fig. 3a shows that not only thermal decomposition temperature but also pyrolysis volatile and solid product yields are directly related to the chemical structure of the pyrolysis material.

When the DTG curves of TLBW, hemicellulosic fraction, and cellulose fraction presented in Fig. 3b were examined, it was determined that the first different peaks formed at 269 °C, 210 °C, and 238 °C, respectively. The first peak for TLBW was probably due to the thermal degradation of hemicellulose. The cellulose macromolecule (straight and long-chain consisting of glucose monomers) within the raw tea brewing waste underwent thermal decomposition in the temperature range of 326–364 °C, and maximum weight loss was achieved at 343 °C. Depending on the depolymerization and glycosidic binding of the main components of the lignocellulosic structure, the time-dependent weight reduction rate peaked in the range of 300–400 °C. It was observed that the lignin fraction within the raw tea leaf brewing waste showed degradation

over a wide temperature range; therefore there were no clear boundaries for the decomposition temperatures of the main components. The degradation zones and temperature ranges obtained from the thermograms are summarized in Table 3.

The zone where thermal degradation was observed (200–610 °C) was divided into two zones for both the raw tea brewing waste and the principal components (hemicellulose and cellulose fractions) obtained through isolation. For the TLBW, hemicellulose, and cellulose fractions in the first zones, T_i values were considered 269, 210, and 238 °C, while T_p and T_f temperatures were 343, 291, and 319 °C and 364, 371, and 379 °C, respectively. In the second zone, T_i, T_p, and T_f temperatures were seen as 387, 376, and 384 °C; 410, 451, and 471 °C; and 602, 527, and 531 °C, respectively.

3.4 Kinetic and thermodynamic analysis

As a result, it was demonstrated by thermal degradation curves (behaviors) of the isolated fractions that the thermal stability of cellulose was higher than that of hemicellulose. The obtained results are in accordance with those in the literature [11, 59].

Table 3 TGA-DTG characteristic parameters of TLBW and its main component

	Characteristic properties	TLBW	TLBW-H	TLBW-C
Zone 1 (40–150 °C)	T_i(°C)	48.98	48.98	48.98
	T_f(°C)	153.8	138.52	142.66
	T_p(°C)	99.42	85.55	103.0
	DTG_p(µg/min)	0.1960	2.6698	0.1942
Zone 2 (200–380 °C)	T_i(°C)	269.28	210.57	238.52
	T_f(°C)	364.40	371.04	379.19
	T_p(°C)	343.67	291.84	319.83
	DTG_p(µg/min)	0.1415	0.5247	0.1411
Zone 3 (380–610 °C)	T_i(°C)	387.13	376.08	384.99
	T_f(°C)	602.61	527.16	531.28
	T_p(°C)	410.49	451.02	471.46
	DTG_p(µg/min)	0.1410	0.3536	0.1379

Kinetic and thermodynamic parameters are of critical importance on an industrial scale in terms of process and reactor design [62]. In this study, kinetic (exponential factor and activation energy) and thermodynamic calculations (enthalpy, entropy, free energy) were performed for the temperature range of 200–610 °C, which included the second and third thermal degradation steps where major weight loss occurred. Coast–Redfern method, which is based on integral analysis and widely used by many researchers, was preferred for kinetic analysis. The activation energy, considered to be a measure of the reaction reactivity and defined as the minimum energy required to initiate a chemical reaction [63], was calculated using different solid-phase theoretical model equations and presented in Table 4. The regression coefficients of the linear equations obtained from the graphs drawn for different solid-phase theoretical model equations using the Coast-Redfern method are presented in Table 4. It was concluded that the kinetic model equation with the regression coefficient closest to one was the solid-phase decomposition theoretical kinetic model equation that best describes the decomposition process. As seen in Table 4, the regression coefficients were between 0.5 and 0.95. It was determined that the chemical kinetic F(3) mechanism best described the degradation step for both the raw tea brewing waste and the hemicellulose and cellulose fractions recovered from this waste. For the best suitable model equation, the regression coefficients of TLBW, TLBW-C, and TLBW-H were determined as 0.939, 0.964, and 0.932, respectively. The average activation energy and ln (A min^{-1}) values calculated by considering the most appropriate model equation were calculated as 46.715, 23.838, and 14.424 kJ/mol and 10.437, 13.205, and 14.095 kJ/mol, respectively.

The studies in the literature have reported that the magnitude of A* varies according to the reaction types in the pyrolysis process [64]. When the A* value is $< 10^9$ s^{-1} or in between 10^{10} and 10^{12} s^{-1}, the pyrolysis takes place as only the surface reaction or decomposition of cellulose, respectively. The value higher than 10^{14} s^{-1} infers a high number of molecule collisions, which means that the pyrolysis process needs high activation energy [65].

All of the A* varies obtained in the study were less than $< 10^9$ s^{-1}; for this reason, it was concluded that the pyrolysis of TLBW and the main component were taken place only as a surface reaction. A* similar result was obtained in the study conducted by Yaraş et al. (2021) [66], on the thermal transformation behavior of paper mill sludge. The calculated thermodynamic parameters for all of the theoretical model equations are presented in Table 5. Enthalpy (ΔH) is a state function that shows whether the reaction is exothermic or endothermic [67]. It reflects the energy of decomposition of chemical bonds under constant pressure. The ΔH values of TLBW, TLBW-H, and TLBW-C using the best suitable model equation (chemical kinetic (F3)) were calculated as 41.593, 18.999, and 9.735 kJ mol^{-1}, respectively. ΔH values calculated according to the whole model equation were positive.

This result indicates that the pyrolysis of TLBW and its main component under the nitrogen atmosphere was endothermic. Hence, it was revealed that it needed external energy [66]. As seen in Table 5, the calculated ΔH values for all model equations were higher for raw tea brewing waste. This is thought to be due to the lignin content of the raw waste. The high ΔH values in raw tea brewing waste were due to the lignocellulosic structure containing strong chemical bonds. It is known that these bonds are broken in processes of isolation of key components (alkali pretreatment processes). The finding is a result of the alkaline processes applied in the insulation process in this context. During alkaline pretreatment processes, generally, the size of lignocellulosic biomass resources decreases, their physical structure is opened, lignin and hemicellulose are removed from biomass, the crystallinity of cellulose is reduced, and the porous structure is increased. Gibbs free energy (ΔG) determines when a chemical reaction naturally occurs and the course of the reaction [68, 69]. ΔG values calculated by considering different theoretical model equations are presented in Table 5. The calculated ΔG values for the raw tea brewing waste and its main components were very close to each other.

Entropy (ΔS) is an indicator of irregularity degree. The examination of the values presented in Table 5 reveals that the entropy values were calculated negatively for all theoretical model equations. This result indicates that the degree of irregularity increased due to the volatile components released during thermal degradation of the sample. The degree of irregularity of the products as a result of the process was higher than that of reactants.

Table 4 Activation energy and coefficient estimates according to Coast–Redfern Method

Model	Parameters	TLBW	TLBW-C	TLBW-H
Chemical kinetics F (0)	E (kJ/mol)	9.737	6.788	4.907
Power law (P1)	Ln(A min^{-1})	14.411	14.828	14.933
One-dimensional interaction geometry (R1)	R^2	0.632	0.595	0.577
Chemical kinetics (1/2)	E (kJ/mol)	18.359	11.450	6.225
Interaction geometry in cylindrical system (R2)	Ln(A min^{-1})	14.106	14.194	15.497
	R^2	0.718	0.810	0.691
Chemical kinetics (2/3)	E (kJ/mol)	19.722	8.990	6.688
Interaction geometry spherical system (R3)	Ln(A min^{-1})	14.256	15.253	15.847
	R^2	0.743	0.721	0.722
Chemical kinetics F(1)	E (kJ/mol)	22.685	9.781	7.651
	Ln(A min^{-1})	12.592	15.546	14.617
	R^2	0.791	0.754	0.776
Chemical kinetics F(2)	E (kJ/mol)	33.467	17.151	10.827
	Ln(A min^{-1})	10.437	13.205	14.095
	R^2	0.891	0.911	0.880
Chemical kinetics F(3)	E (kJ/mol)	46.715	23.838	14.424
	Ln(A min^{-1})	7.669	11.916	13.407
	R^2	0.939	0.954	0.932
Parabolic law (D1)	E (kJ/mol)	40.173	24.321	19.834
	Ln(A min^{-1})	11.297	13.857	14.635
	R^2	0.774	0.845	0.874
Holt–Cutler–Wadsworth equation (D2)	E (kJ/mol)	44.626	27.101	21.523
	Ln(A min^{-1})	11.015	13.961	14.939
	R^2	0.802	0.871	0.891
Jander equation (D3)	E (kJ/mol)	50.165	28.165	23.396
	Ln(A min^{-1})	11.310	15.240	16.008
	R^2	0.833	0.880	0.907
Ginstling–Brounshtein equation (D4)	E (kJ/mol)	46.452	30.307	22.146
	Ln(A min^{-1})	12.122	14.783	16.299
	R^2	0.813	0.895	0.897

4 Conclusions

In this study, thermal degradation behaviors and pyrolysis kinetics of the TLBW and its main components (hemicellulose and cellulose) which were isolated using the alkaline pretreatment method from TLBW were investigated using thermogravimetric analysis.

The thermal decomposition process for raw tea brewing waste involved two main stages. In the first stage, the hemicellulose and cellulose biopolymers were degraded, which was called the active zone, and the lignin polymer was degraded in the second stage, which was called the passive zone. TG-DTG curves confirmed that the thermal stability of hemicellulose was lower than cellulose and crude sample. The degradation peak of the raw sample shifted towards the higher region than cellulose and hemicellulose. The thermal decomposition temperature of the main isolated components decreased. This was interpreted as a result of the lignin content of the raw tea brewing waste.

In the physicochemical analysis of the raw material and the basic components obtained from this raw material, it was determined that the bioenergy potential was high. FTIR analysis results proved that the raw material could be separated effectively and the delignification process success was high.

Based on the kinetic analysis, it was revealed that the pyrolysis results fit the chemical kinetic F(3) model. The experimental data are of great importance in terms of optimization of pyrolysis conditions, industrial-scale reactor, and process design. As a result, tea brewing waste and its basic components are a potential energy source that can be used in sustainable and clean energy production with both reserve potential and energy potential aspects.

Table 5 Thermodynamic parameter estimate according to the best suitable model equation

Model	Parameters	TLBW	TLBW-C	TLBW-H
Chemical kinetics F (0)	ΔH(kJ/mol)	4.616	1.949	0.218
Power law (P1)	ΔG(kJ/mol)	54.152	53.435	53.696
One-dimensional interaction geometry (R1)	ΔS(kJ/molK)	−0.080	−0.088	−0.095
Chemical kinetics (1/2)	ΔH(kJ/mol)	13.238	6.611293	1.536
Interaction geometry in cylindrical system (R2)	ΔG(kJ/mol)	50.904	50.904	52.581
	ΔS(kJ/molK)	−0.061	−0.076	−0.091
Chemical kinetics (2/3)	ΔH(kJ/mol)	14.600	4.151	1.999
Interaction geometry spherical system (R3)	ΔG(kJ/mol)	50.538	52.075	52.244
	ΔS(kJ/molK)	−0.058	−0.082	−0.089
Chemical kinetics F(1)	ΔH(kJ/mol)	17.563	4.942	2.962
	ΔG(kJ/mol)	49.821	51.667	51.614
	ΔS(kJ/molK)	−0.052	−0.080	−0.086
Chemical kinetics F(2)	ΔH(kJ/mol)	28.346	12.312	6.138
	ΔG(kJ/mol)	47.829	48.949	49.985
	ΔS(kJ/molK)	−0.032	−0.063	−0.078
Chemical kinetics F(3)	ΔH(kJ/mol)	41.593	18.999	9.735
	ΔG(kJ/mol)	46.121	47.356	48.641
	ΔS(kJ/molK)	−0.007	−0.049	−0.069
Parabolic law (D1)	ΔH(kJ/mol)	35.052	19.482	15.145
	ΔG(kJ/mol)	46.894	47.259	47.147
	ΔS(kJ/molK)	−0.019	−0.048	−0.057
Holt–Cutler–Wadsworth equation (D2)	ΔH(kJ/mol)	39.505	22.262	16.834
	ΔG(kJ/mol)	46.355	46.735	46.764
	ΔS(kJ/molK)	−0.011	−0.042	−0.053
Jander equation (D3)	ΔH(kJ/mol)	45.044	23.327	18.707
	ΔG(kJ/mol)	45.756	46.549	46.373
	ΔS(kJ/molK)	−0.001	−0.040	−0.049
Ginstling–Brounshtein equation (D4)	ΔH(kJ/mol)	41.331	25.468	17.457
	ΔG(kJ/mol)	46.150	46.195	46.630
	ΔS(kJ/molK)	−0.008	−0..036	−0.052

References

1. Wang X, Deng S, Tan H, Adeosun A, Vujanović M, Yang F, (2016) Duić N Energy Convers Manag 118, 399–405
2. Jin J, Li Y, Zhang J, Wu S, Cao Y, Liang P, Zhang J, Wong MH, Wang M, Shan S, Christie P, (2016) J Hazard Mater 320, 417–426
3. Naqvi SR Ali, I. Nasır, S. Ali Ammar Taqvi S, Atabani AE, Çetin W-H. (2020) Fuel 278:118259.
4. Bajpai P (2016) Structure of lignocellulosic biomass. In: Pretreatment of lignocellulosic biomass for biofuel production. SpringerBriefs in Molecular Science. Springer, Singapore.
5. Houfani, A. A., Anders, N., Spiess, A. C., Baldrian, P., Benallaoua, S. (2020) Biomass and Bioenergy, 134:Article 105481.
6. Cherif MF, Trache D, Brosse N, Benaliouche F, Tarchoun AF (2020) Waste Biomass Valor:1–13
7. Liao JJ, Latif NHA, Trache D, Brosse N, Hussin MH (2020) Int J Biol Macromol. 162:985–1024. https://doi.org/10.1016/j.ijbiomac.2020.06.168
8. Gouws SM, Carrier M, Bunt JR, Neomagus HWJP (2021)Renew Sust Energ Rev 135:Article 110189.
9. Zhang S, Su Y, Xu D, Zhu D, Zhang H, Liu X, (2018)Energy, 149, 804-813.
10. Álvarez C, Reyes-Sosa FM, Díez B, (2016) Microbial Biotechnol, 9 (2) :149-156,
11. Wang S, Dai G, Yang H, Luo Z. (2017) Prog energy combust Sci 62:33-86.
12. Müsellim E, Tahir MH, Ahmad MS, Ceylan S, (2018), Appl Therm Eng 137:54–61.
13. Nowicki L, Ledakowicz SJ (2014) Anal Appl Pyrolysis 110:220–228

14. Dhyani V, Kumar J and Bhaskar T, (2017) Bioresour. Technol., 245:1122-1129.

15. Çaykur enterprises raport, (2019), http://biriz.biz/cay/istatistikler.htm [accessed 20 Feb 2020]

16. Global tea statistics report (2019), https://www.statista.com/statistics/507950/global-per capita-tea-consumption-by-country/ [accessed 15 Jan 2019]

17. Aslan DI, Özoğul B, Ceylan S, Geyikçi F (2018) Bioresour Technol 258 105–110.

18. Ceylan S, Topçu Y (2014) Bioresour Technol 156:182–188

19. Orfao J, Antunes F, Figueiredo J, (1999) Fuel 78 (3), 349–358.

20. Kaur R, Gera P, Jha MK, Bhaskar T, (2018) Bioresour Technol. 250:422–428.

21. Herbaut M, Zoghlami A, Habrant A, Falourd X, Foucat L, Chabbert B, Paës G, Biotechnol Biofuels 11 1-17.

22. Han Y, Bai Y Zhang J, Liu D, Zhao X, (2020)Bioresour Bioprocess 7 1-16.

23. Nan Y, Jia L Yang M Xin D Qin Y Zhang J, (2018) Bioresour. Technol. 261 223–231.

24. ASTM-E 872. (1982) Volatile matter in the analysis of particulate wood fuels. Annual Book of ASTM Standards.

25. ASTM-E 1755. (1995) Ash in biomass. Annual Book of ASTM Standards.

26. Li S, Xu S, Shuqin L, Chen Y, Qinghua L, (2004) Fuel Process Technol 85 1201-1211.

27. Sadhukhan AK, Gupta P, Saha RK (2009) Bioresour Technol 100: 3134–3139.

28. Ali I Tariq R, Naqvi SR, Khoja AH, Mehran MT, Naqvi M, Gao N, (2021) J Energy Instit 95:30-40.

29. Coats, A., Redfern, (1964) J. Nat 201:68–69.

30. Ali I (2018) Bioresour Technol Rep 2:88–91

31. Vuppaladadiyam AK, Liu H, Zhao M, Soomro AF, Memon MZ, Dupont V. (2019) Biotechnol Biofuels 12:1-18.

32. Kumar M., Mishra P.K., Upadhyay S.N., (2020) Fuel, 268:117164.

33. He Y, Chang C, Li P, Han X, Li, Fang S, Chen J, Ma X (2018) Bioresour Technol 259:294–303

34. He Q, Ding L, Gong Y, Li W, Wei J, Yua G, (2019), Bioresour Technol 280:104–111.

35. Rony AH, Kong L, Lu W, Dejam M, Adidharma H, Gasem KAM, Zheng Y, Norton U, Fan M, (2019) Bioresour Technol 284, 466–473.

36. Tang Q; Chen Y; Yang H; Liu M; Xiao H; Wu Z; Chen H; Naqvi SR (2020) Energy Fuels 34 (9):11050−11060.

37. Lawal AI, Aladejare AE, Onifade M Bada S, Adebayo M, ANN and MLR. (2021) Int J Coal Sci Technol 8:124–140.

38. García R, Pizarro C, Lavín AG, Bueno JL, (2014) 117:1139–1147.

39. Demirbas A, (2002) Energy Exploration & Exploitation 20(1), 105-111.

40. Mohan D, Pittman CU, Steele PH (2006) Energy Fuel 20:848–889

41. Demirbas A, (2017) Energy Sources, Sart A: Recover Utılızatıon Envıron Effects, 39(6):592–598.

42. Gómez-Martína JM, Castaño-Díaz M, Cámara-Obregón A, Álvarez-Álvarez, Folgueras-Díaz MB, Diezc MA, (2020) Energy Rep, 6:764–76.

43. Goutam SG, Monoj KG, Mondal K.(2019), Energy, 181:665-676.

44. Perea-Moreno MA, Manzano-Agugliaro F, Hernandez-Escobedo Q, Perea-Moreno AJ (2018) Sustainability 10:3254

45. Wang K, Wang B, Hu R, Zhao X, Li H, Zhou G, Song L, Wu A, (2019) Carbohydr Polym. 221:127-136.

46. Samanta AK, Senani S, Kolte AP, Sridhar M, Sampath KT, Jayapal N, Devi A, (2012) Food Boprod Proc 90:466–474.

47. Sun XF, Jing Z, Fowler P, Wu Y, Rajaratnam M (2011) Ind Crop Prod 33:588–598

48. Tutuş A, Kazaskeroğlu Y, Çiçekler M, (2015) BioResources 10 (3): 5407-5416.

49. Pirbazari AE, Pargami NR, Ashja N,.Emami MS, (2015) J Environ Anal Toxicol 5(5) 1-11.

50. Brienzo M, Siqueira AF, Milagres, AMF (2009) Biochem Eng J, 46:199–204

51. Buranov AU ve Mazza, G (2008), Industrial Crops Products, 28: 237-259.

52. Sun X-F, Jing Z, Fowler P, Wu YM, (2011) Industrial Crops Prod 33:588–598

53. Egüés I, Eceiza A, Labidi J. (2013) Industrial Crops Prod 47:331-338.

54. Seki Y, Sarıkanat M, Sever K, Durmuşkahya C (2013) Composites: part B, 44 (1):517-523.

55. Rahman M, Rahman R, Hamdan S, Hossen F, Lai JCH, Liew FK, (2015) Int J Polymer Sci, 3:1-4

56. Bulut Y, Aksit A (2013) Cellulose 20(6):3155–3164

57. Mandal A and Chakrabarty D (2011) Carbohydr Polym. 86:1291-1299.

58. Lan W, Liu C-F, Sun RCJ (2011) Agric Food Chem 59:8691–8701

59. Demirbaş A, (2004) J Anal Appl Pyrolysis 72:243-248.

60. Vigourox RZ (2001) Pyrolysis of biomass, Kungly Tekniska Högskolan, Royal Institute of Technology, Doctoral thesis, Department of Chemical Engineering and Technology. Chem Technol 144:1104–3466 Stockholm

61. Yaman S (2004) Energy Convers Manag 45:651–671

62. Xiao R, Yang W, Cong X, Dong K, Xu J, Wang D, Yang X. (2020) Energy 201:117537.

63. Chen J, Liu J, He Y, Huang L, Sun S, Sun J, Chang KL, Kuo J, Huang S, Ning X (2017) Bioresour Technol 225:234–245

64. Yuan X, He T, Cao H, Yuan Q, (2017)Renew Energy 107:489–496

65. Xu Y, Chen B, (2013), Bioresour Technol 146:485–493

66. Yaras A, Demirel B, Akkurt F Arslanoğlu H, (2021) Biomass Conv Bioref.. https://doi.org/10.1007/s13399-020-01232-9

67. Kim YS, Kim YS, Kim SH (2010) Environ Sci Technol 44:5313–5317

68. Khan AS, Man Z, Bustam MA, Kait CF, Ullah Z, Nasrullah A, Khan MI, Gonfa G, Ahmad P, Muhammad N, (2016) J Mol Liq. 223:754–762.

69. Cai Q, Fan Z, Chen J, Guo W, Ma F, Sun S, Zhou Q, (2018) J Mol Struct 1171:639–643.